Lawrence Berkeley Laboratory
UNIVERSITY OF CALIFORNIA
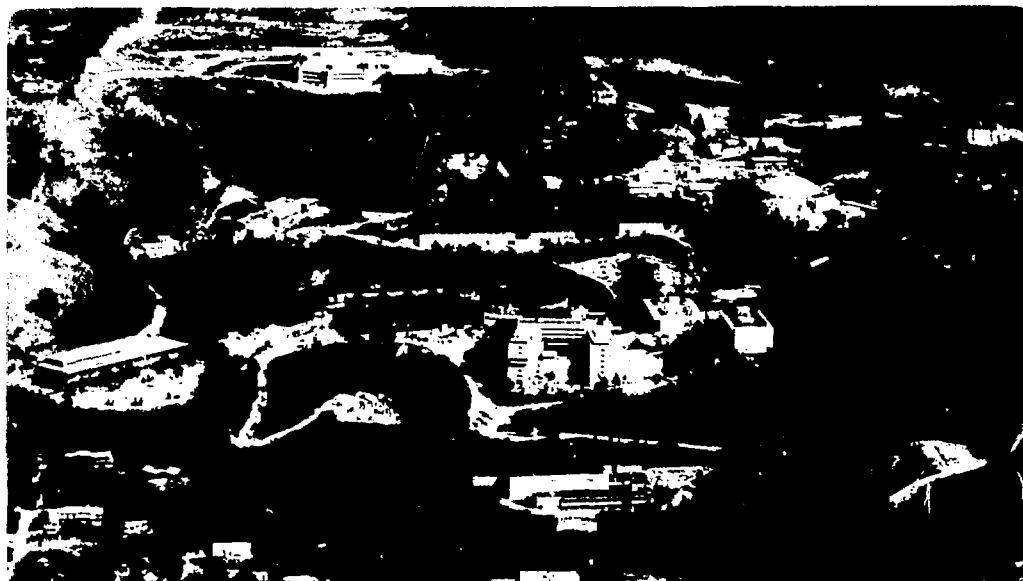
Engineering Division

**MLE Reconstruction of a Brain Phantom
Using a Monte Carlo Transition Matrix
and a Statistical Stopping Rule**

E. Veklerov, J. Llacer, and E.J. Hoffman

October 1987

DISCLAIMER

MLE RECONSTRUCTION OF A BRAIN PHANTOM USING A MONTE CARLO
TRANSITION MATRIX AND A STATISTICAL STOPPING RULE

Eugene Veklerov and Jorge Llacer
Lawrence Berkeley Laboratory, University of California
Berkeley, California 94720 U.S.A.

Edward J. Hoffman
Dept. of Radiological Sciences, School of Medicine
University of California, Los Angeles
Los Angeles, California 90024 U.S.A

ABSTRACT

In order to study properties of the Maximum Likeli-
hood Estimator (MLE) algorithm for image reconstruction
in Positron Emission Tomography (PET), the algorithm is
applied to data obtained by the ECAT-III tomograph from
a brain phantom. The procedure for subtracting acci-
dental coincidences from the data stream generated by
this physical phantom is such that the resultant data
are not Poisson distributed. This makes the present
investigation different from other investigations based
on computer-simulated phantoms. It is shown that the
MLE algorithm is robust enough to yield comparatively
good images, especially when the phantom is in the pe-
riphery of the field of view, even though the underly-
ing assumption of the algorithm is violated. Two tran-
sition matrices are utilized. The first uses geometric
considerations only. The second is derived by a Monte
Carlo simulation which takes into account Compton scat-
tering in the detectors, positron range, etc. in the
detectors. It is demonstrated that the images obtained
from the Monte Carlo matrix are superior in some speci-
fic ways. A stopping rule derived earlier and allowing
the user to stop the iterative process before the im-
ages begin to deteriorate is tested. Since the rule is
based on the Poisson assumption, it does not work well
with the presently available data, although it is suc-
cessful with computer-simulated Poisson data.

INTRODUCTION

Iterative image reconstruction algorithms have been
widely discussed in literature on Positron Emission
Tomography. In particular, the MLE algorithm is re-
ceiving substantial attention since it has a number of
advantages over other reconstruction schemes. However,
it has not been sufficiently tested to clearly under-
stand its properties. To this end, we apply the MLE
algorithm to reconstruction of a brain phantom. Unlike
computer-simulated phantoms used in most of the studies
of the MLE algorithm, our data was generated by the
ECAT-III tomograph, as described by Hoffman et al[1].
Figure 1 shows the geometry of the source. The ratio
of activities between the regions in black and those
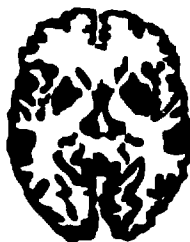in white in the interior of the phantom is ~ 4:1.

Fig. 1: Drawing of the brain phantom. The ratio of
activities between the regions in black and those in
white in the interior of the phantom is ~ 4:1.

One aspect of the data acquisition process of
ECAT-III that we used may have ramifications on the
applicability of the MLE algorithm. In order to remove
random coincidences, the method of prompt vs. delayed
coincidences was used[2]. According to this method,
random coincidences in every detector pair are sub-
tracted from the total number of coincidences in that
same pair. In the case of our data, the subtraction
was carried out on line, during image acquisition.
The two measurements are taken over disjoint intervals
of time so that they are probabilistically independent.

It is reasonable to assume that the results of both
measurements are Poisson distributed. It is known that
while the sum of two independent Poisson random vari-
ables is Poisson distributed, the difference is not.
Since the MLE algorithm expects only non-negative val-
ues, we truncated the negative values to zero, which,
however, did not make the data Poisson distributed.

Thus, we have encountered a situation where the
main premise of the MLE algorithm that the number of
detected coincidences in any detector pair is a Pois-
son variable is violated. It is interesting to see
what images are reconstructed by the MLE algorithm in
this case and to observe the behavior of a stopping
rule for the MLE algorithm that we have published re-
cently[3]. This rule is based on the simple statisti-
cal consideration that the image reconstructed should
have been able to generate the set of coincidence data
by a Poisson process with a high confidence level.
This paper will present the results of these two sets
of observations.

COMPUTATION OF TRANSITION MATRICES

The central part of the MLE algorithm is the tran-
sition matrix which is a set of the probabilities
$p(b,d)$ that a gamma pair emitted from the pixel b is
detected by the detector pair d. When computer simu-
lated data is used for reconstruction, the choice of
$p(b,d)$ is not crucial, as long as the same matrix is
used for both simulation and reconstruction. However,
when data is generated by a physical instrument, the
matrix used for reconstruction should reflect the real
probabilities controlling the physical experiment.

The earliest transition matrix was reported by
Shepp and Vardi[4]. It is based on some simplified
geometric considerations. This matrix has been com-
pared with another transition matrix that takes into
account Compton scattering, detection efficiency, pres-
ence of absorbers, positron range and non-colinearity
of gamma-pairs. The computation uses a Monte Carlo
simulation package called EGS4 described by Nelson et
al[5]. The generation of transition matrices by con-
sidering the physical properties of the detectors has
been used by Llacer et al[6,7] for small positron emis-
sion cameras and by Floyd et al[8] for SPECT.

EGS4 is a general purpose package for simulating
the interactions of electrons and photons in arbitrary
geometry and materials. It has been adapted to the

UCLA 512-crystal (BiGeO) ring described by Hoffman et al[1]. The computation proceeds as follows. We start out at a given source point. Then we generate a random annihilation point using the positron range distribution derived by Derenzo[9]. The first photon is emitted from the annihilation point in a uniformly distributed random direction. Due to a residual energy at annihilation, the angle between the first photon and the second may deviate from 180°. (For the emission angle distribution see Colombino et al[10]). The two photons travel in straight lines and if both hit the detector ring, their further trajectories are taken over by EGS4 which also computes the amount of energy deposited by a photon in any detector. A photon which deposits more energy in a detector than a given threshold is said to be "detected", provided that it is detected by only one detector (multiple detections are vetoed). If both photons of a pair are detected, this event increments the corresponding element of a matrix which becomes the transition matrix after normalization. A pixel is approximated by a set of source points.

A sample of simulation results is presented in Fig. 2. It depicts the numbers of pairs detected by vertical tubes as the source point moves along the horizontal diameter in the right semicircle. A vertical tube is defined as the space between two parallel lines that join the edges of detectors placed symmetrically about the horizontal diameter. The tubes are numbered from 1 (the tube covering the vertical diameter) to 128 (the rightmost vertical tube). Short vertical lines mark the tube boundaries in the figure. Crosses show the numbers of detected pairs as a function of the x-coordinate of the source. Fig. 2a) shows the results for tubes 1 and 2 and Fig. 2b) for tubes 40 and 41. Due to the ring geometry, peripheral tubes are narrower than central ones. Furthermore, the detector faces are not perpendicular to peripheral vertical tubes. Therefore, the probability that a vertical pair of photons will be detected is significantly lower for peripheral tubes than for central ones. Another effect that can be observed is that this response function is less sharp in case of peripheral tubes and the maximum of the response function shifts to the right with respect to the center of the tube. This effect is also caused by the ring geometry and the finite absorption coefficient of the detector material. The response functions obtained by simulation are then approximated by smooth functions characterized by several parameters. These smooth functions are shown in Fig. 2 as well. They make up a "database" that is used to generate a transition matrix. Images reconstructed with the "Shepp-Vardi" transition matrix are compared with those reconstructed with the "Monte Carlo" matrix below.

STOPPING RULE

Several authors have observed that as the MLE iterative process passes a certain point, the reconstructed images exhibit strong deterioration. This phenomenon has been explained from different viewpoints and several remedies have been proposed. Snyder et al[11] noticed that this effect is fundamental to the application of unconstrained maximum likelihood estimation. We would like to take a step further.

Let $n(d)$ $(d = 1, \ldots D)$ be the projection data, i.e., the number of coincidences detected in tube d and $\lambda(b)$ $(b = 1, \ldots B)$ the emission density in pixel b. Consider an algorithm which tries to minimize the differences between $n(d)$ and

$$\lambda^*(d) = \sum_b p(b, d) \lambda(b) \qquad (1)$$
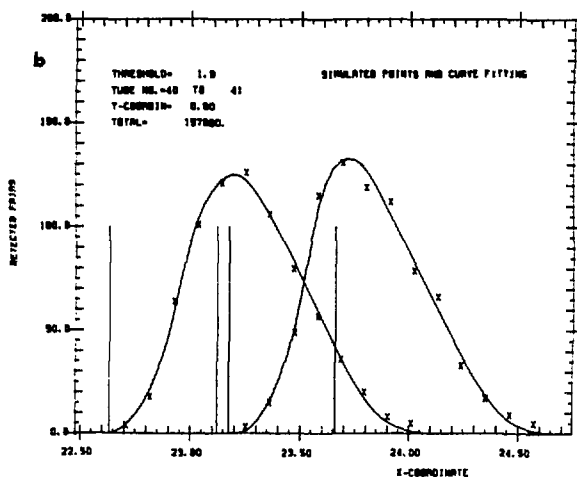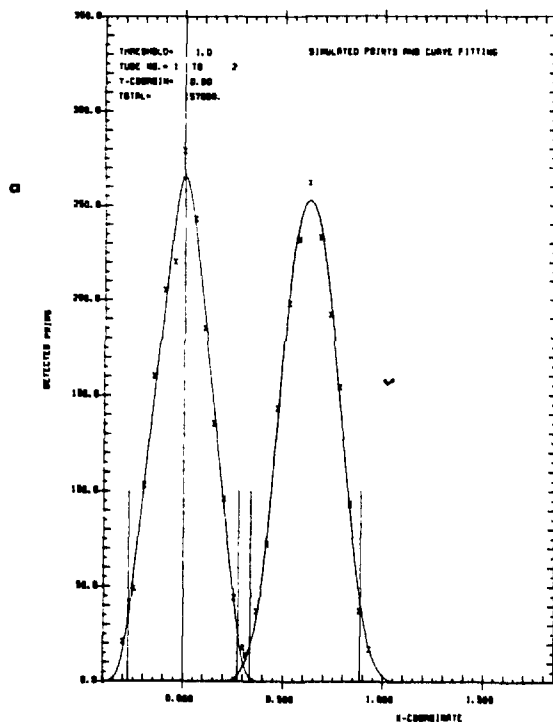
in some sense.

XBL 8710-4269

XBL 8710-4267

Fig. 2: Simulation results: the response function for a few tubes when the source point moves along the horizontal diameter: a) tubes 1 and 2; b) tubes 40 and 41. The crosses are actual simulation points; smooth curves are their approximations.

The attainment of the maximum likelihood solution is but one approach to the goal of minimizing the differences. Another approach that immediately comes to mind is minimizing the sum of the squares of the differences. Llacer and Veklerov proposed yet another criterion for research purposes which was called "weighted maximum likelihood"[12]. It was later pointed out by Veklerov and Llacer[3] that the eventual

deterioration of images is fundamental to the application of unconstrained minimization of the differences, not only by the MLE method.

Indeed, suppose we are able to recover an image, such that n(d) and λ*(d) are very close. If they are too close, this may be inconsistent with the physical nature of the experiment, whereby each n(d) is a realization of a Poisson variable with the mean λ*(d). For instance, the Poisson distribution calls for a specific deviation of n(d) from λ*(d), which is specifically the square root of λ*(d). As a result of unconstrained minimization, the deviation may become less than that value. In that case, a source distribution identical to the recovered image could not have possibly generated the data.

The specific visual form by which continued iteration degrades an image after a certain point will depend on the nature of the function whose extremum is being sought. The MLE is particularly badly behaved, although we have been able to modulate the degradation effect with respect to accurate reconstruction of areas of low level activity by a Weighted Likelihood function[12].

The above facts were used by Veklerov and Llacer[3] for formulating a stopping rule for iterative processes. According to the rule, we test the hypothesis that the projection data is a (scaled) Poisson sample drawn from the distribution determined by the image obtained after each iteration. The iterative process stops when the hypothesis can be accepted (or rather, not rejected). We emphasize that the requirement that the recovered image be consistent with the Poisson nature of the measurements has nothing to do with the specific criterion used by Shepp and Vardi[4] to derive the MLE algorithm. Since the requirement results from the physical nature of the experiment, it follows that it is applicable to any iterative process based on any criterion that tries to match the data and reconstructed images. Although it cannot be guaranteed that any iterative process will pass through "acceptable" images, the occurrence of this passage is sufficient for stopping the iterative process. So far we have observed that for all data sets generated in accordance with the Poisson assumption, the MLE algorithm does pass through acceptable images.

Defrise[13] proposed another stopping rule based on Morozov's discrepancy principle that "the estimated solution should not fit the data with an accuracy greater than the accuracy of the measurement". This principle is a general statement of the idea that motivated our research. Unlike the principle proposed by our group, however, this principle and its realization proposed by Defrise do not take into account the specific statistical nature of the measurements.

Returning to the brain phantom, since its n(d) are not Poisson-distributed, our stopping rule in its present form is not directly applicable. Veklerov and Llacer[3] defined a parameter denoted H which is a quantitative measure of how close the distribution of scaled n(d)'s is to a Poisson distribution. In "normal" cases, H reaches a clear minimum and then gradually increases. Figure 3, lines a and b, show the hypothesis testing parameter H for a computer simulated brain phantom in which the data were Poisson distributed, for 1 million and 4 million counts, respectively[14]. The horizontal line d indicates the value of H below which we can have 99 % confidence that the image iteration tested could have generated the data by a Poisson process. In the present case, line c, H does not pass through a minimum, nor does it become low enough to pass the Poisson test. Thus, the stopping
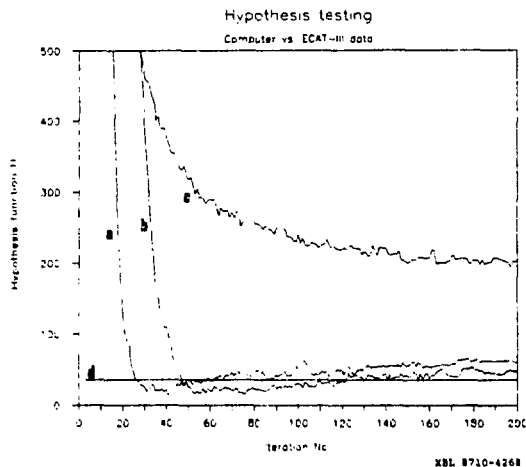

Fig. 3: Hypothesis testing function H for computer simulated and physical brain phantoms: a) Computer simulated, 1M counts; b) ditto, 4M counts; c) physical phantom, 1M counts.

rule, in its present form, is not capable of capturing the "best" image for data that are not Poisson distributed initially.

Since the prompt vs. delayed coincidence method of subtracting random coincidences is a very elegant way of generating clean data in the less-than-ideal timing resolution BiGeO detector systems, we have recently obtained individual coincidence data for the prompt and the delayed coincidence events of the present brain phantom for the purpose of studying the best way of reconstructing those images by MLE methods.

DISCUSSION OF RECONSTRUCTED IMAGES

The purpose of this section is to compare images reconstructed with the filtered back-projection (FBP) algorithm using the Hanning window with those reconstructed with the MLE algorithm using the transition matrix proposed by Shepp and Vardi[4] (SV), as well as the transition matrix derived from the Monte Carlo simulation (MC) described above. Since the difference between the SV matrix and the MC matrix is most pronounced for the peripheral tubes, the phantom was placed first at the center of the detector circle and then at the lower edge by displacing its center by 15.5 cm. The data sets generated in these two experiments were used for reconstruction.

Figure 4 depicts the FBP reconstructions of the brain phantom located at the center (a) and at the edge (b) when the total number of counts is 1 million (1M). Both images were initially reconstructed at 256 x 256 pixels, with a pixel dimension of 3.05 mm, the natural sampling distance of the ECAT-III. For presentation, a 64 x 64 section has been extracted from the center or edge of the reconstructed results and presented as a centered image. This presentation technique will be used throughout this paper.

Figure 5 compares the center (a) vs. edge (b) images for the MLE reconstructions with the same data as Fig. 4 (1M counts). The center reconstruction shown was carried out with the SV matrix, while the edge image resulted from the MC matrix. In both cases the results after 30 iterations are shown. The hypothesis
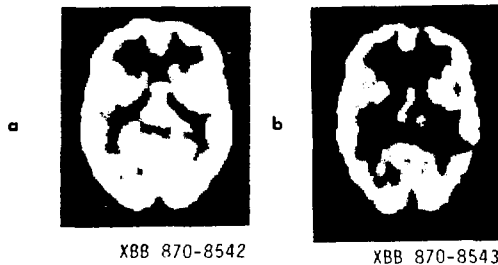
XBB 870-8542   XBB 870-8543

Fig. 4: FBP reconstructions (Hanning window) when the phantom shown in Fig. 1 is a) at the center of the detector circle, b) at the edge. The total number of counts is 1M.

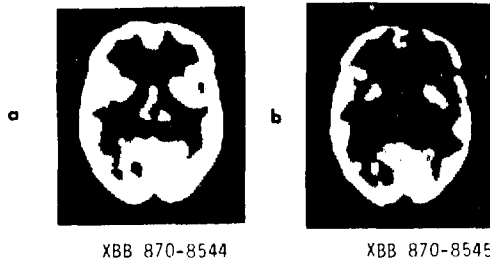XBB 870-8544   XBB 870-8545

Fig. 5: Same images as in Fig. 4, reconstructed by the MLE: a) SV matrix, center region; b) MC matrix, edge region. Both 1M counts, 30 iterations.

testing function H of Fig. 3, line a, and the reconstruction experiments with the simulated brain phantom[14] indicated to us that, with 1M counts, 30 iterations should be close to the "best" image, resulting in a compromise between increased sharpness and deterioration in the regions of uniform density. In the present reconstructions with non-Poisson real data, iteration 30 also yields satisfactory results using only the image quality criteria.

The use of the MC matrix for the centered phantom does not appear to result in any significant improvement over the SV matrix results, with 1M counts in the image. It is apparent, however, that both MLE images of Fig. 5 are clearer, have less noise and more distinct details than the FBP images of Fig. 4.

Additionally, the MC matrix results at the edge of the field of view have the correct shape and size while the SV and FBP images are distorted. The edge FBP images suffer from a vertical elongation, while the SV images are somewhat foreshortened. Figure 6a) shows the difference between the edge image and the center one obtained by the FBP algorithm. The middle level of gray corresponds to zero difference, darker levels correspond to negative differences, brighter to positive ones. Figure 6b) is the same difference for the MLE MC reconstructions. The elongation effect in the FBP case is very clear. The MC difference image shows a misregistration by approximately one pixel. The level of gray scale for Fig. 6 has been compressed strongly about zero in order to show the differences in a prominent manner. The differences in the SV case are intermediate in magnitude between the two cases shown, but of opposite sign to the MC results.

Finally, Fig. 7 shows reconstructions for edge data with 4 million counts (4M), with the SV matrix (a) and with the MC matrix (b). With the increased number of counts the difference in the detailed contents of the
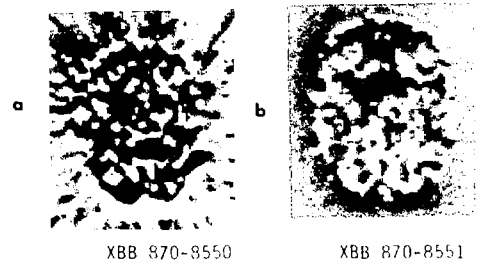

XBB 870-8550   XBB 870-8551

Fig. 6: The difference between the images at the edge and at the center for a) FBP reconstructions, b) MLE reconstructions with the MC matrix.

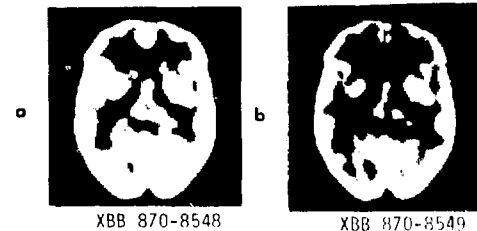XBB 870-8548   XBB 870-8549

Fig. 7: The MLE reconstructions of the edge image, 4M counts, 40 iterations using a) the SV matrix, b) the MC matrix.

images between the two matrices becomes quite evident, particularly on a display with at least 32 levels of gray. With 4M counts, the improvement is also evident with images at the center of the field of view.

In general, the MC transition matrix improves the reconstructed images compared to the ones recovered with the SV matrix. The improvement in shape fidelity occurs at all count levels, while the improvement in detail contents of the images becomes more discernible as the quality of the initial data improves. One would expect that as the resolution of PET tomography improves, the precision of transition matrices will have a greater impact on the quality of reconstructed images, even at low numbers of counts.

A PHILOSOPHICAL CONCLUSION

The MLE algorithm is built on the following premise: the distributions of the counts n(d) are Poisson with the unknown means (d) (d=1, . . . D) and, therefore, it is desirable to maximize the product of the probabilities that each of the D random counts equals n(d), where each probability is a Poisson term with the mean $\lambda^*(d)$. We have shown with our stopping rule work that it is not really desirable to reach a maximization, but that one should stop the iterative process before a contradictory situation arises. If the Poisson nature of the data holds true, the MLE algorithm works in reconstructing data into rather nice images. It may be surprising, however, that the algorithm works even if the Poisson premise does not hold true, as with our present data.

We believe that this is an indication that the specific form taken by the terms of the function to be maximized by the algorithm may be rather flexible. After all, the algorithm simply tries to find an image such that the vectors n(d) and $\lambda^*(d)$ are as close as possible. There are many ways of defining the distance between two vectors and the maximum likelihood criterion is but one of these ways, a way whose merits have

4

been repeatedly demonstrated. Apart from other results, this research raises, but does not answer, the question of whether these merits follow from the underlying assumption that the counts are indeed Poisson-distributed or they have nothing to do with it and the method is merely an optimization technique applicable regardless of the nature of the data.

ACKNOWLEDGMENTS

REFERENCES

1. E.J. Hoffman, A.R. Ricci, L.M.A.M. van der Stee and M.E. Phelps, "ECAT III - Basic Design Considerations", IEEE Trans. Nucl. Sci., NS-30, No. 1, 729-733 (1983).

2. C.W. Williams, M.C. Crabtree and S.G. Burgiss, "Design and Performance Characteristics of a Position Emission Computed Axial Tomograph-ECAT-II", IEEE Trans. Nucl. Sci., NS-26, No. 1, 619-627 (1979).

3. E. Veklerov and J. Llacer, "Stopping Rule for the MLE Algorithm Based on Statistical Hypothesis Testing", IEEE Trans. Med. Imag., MI-6, No. 4 (1987).

4. L.A. Shepp and Y. Vardi, "Maximum Likelihood Reconstruction for Emission Tomography", IEEE Trans. Med. Imag., MI-1, No. 2, 113-121 (1982).

5. W.R. Nelson, H. Hirayama and D.W.O. Rogers, "The EGS4 Code System", Stanford Linear Accelerator Center, SLAC-Report 265 (1985).

6. J. Llacer, A. Chatterjee, H.C. Jackson, J.C. Lin and M.V. Zunzunegui, "An Imaging Instrument for Positron Emitting Heavy Ion Beam Injection", IEEE Trans. Nucl. Sci., NS-26, No. 1, 634-647 (1979).

7. J. Llacer, A. Chatterjee, E.K. Batho and J.A. Poskanzer, "Design Analysis and Performance Evaluation of a Two-dimensional Camera for Accelerated Positron Emitter Beam Injection by Computer Simulation", IEEE Trans. Nucl. Sci., NS-30, 617-625 (1983).

8. C.E. Floyd, R.J. Jaszczak and R.E. Coleman, "Inverse Monte Carlo: A Unified Reconstruction Algorithm for SPECT", IEEE Trans. Nucl. Sci., NS-22, No. 1, 779-785 (1985).

9. S.E. Derenzo, "Precision Measurement of Annihilation Point Spread Distributions for Medically Important Positron Emitters", 5th Inter. Conf. Positron Annihilation, Lake Yamanaka, Japan (1979).

10. P. Colombino, B. Fiscella and L. Trossi, "Study of Positronium in Water and Ice from 22 to -140 C by Annihilation Quantum Measurements", Nuovo Cimento, 38, 707-723 (1965).

11. D.L. Snyder, M.I. Miller, L.J. Thomas and D.G. Politte, "Noise and Edge Artifacts in Maximum-Likelihood Reconstructions for Emission Tomography", IEEE Trans. Med. Imag., MI-6, No. 3, 228-238 (1987).

12. J. Llacer and E. Veklerov, "The High Sensitivity of the Maximum Likelihood Estimator Method of Tomographic Reconstruction", Proc. Inter. Symp. CAR'87, Computer Assisted Radiology, Berlin (1987). Publ. by Springer-Verlag 1987.

13. M. Defrise, "Possible Criteria for Choosing the Number of Iterations in Some Iterative Reconstruction Methods", Proc. NATO Advanced Summer Inst. on Mathematics and Computer Science in Med. Imag., El Ciocco, Italy, Springer-Verlag 1986.

14. J. Llacer and E. Veklerov, "The Maximum Likelihood Estimator Method for Image Reconstruction: Its Fundamental Characteristics and Their Origin", Proc. 10th Information Processing in Med. Imag. (IMPI) Inter. Conf., Utrecht, The Netherlands (1987). Plenum Publishing Corp. 1987.